Magnetic Resonance Imaging in Peripheral Arterial Disease Reproducibility of the Assessment of Morphological and Functional Vascular Status

Please check the document version of this publication:

• A submitted manuscript is the version of the article upon submission and before peer-review. There can be important differences between the submitted version and the official published version of record. People interested in the research are advised to contact the author for the final version of the publication, or visit the DOI to the publisher's website.
• The final author version and the galley proof are versions of the publication after peer review.
• The final published version features the final layout of the paper including the volume, issue and page numbers.

Link to publication

Magnetic Resonance Imaging in Peripheral Arterial Disease

Reproducibility of the Assessment of Morphological and Functional Vascular Status

Bas Versluis, MD,*† Walter H. Backes, MSc, PhD,*† Marcelle G. A. van Eupen, MD,*†
Karolien Jaspers, MSc,*† Patty J. Nelemans, MD, PhD,‡ Ellen V. Rouwet, MD, PhD,§
Joep A. W. Teijink, MD, PhD,¶ Willem P. Th. M. Mali, MD, PhD,‖ Geert-Willem Schurink, MD, PhD,**
Joachim E. Wildberger, MD, PhD,*† and Tim Leiner, MD, PhD*†‖

Objectives: The aim of the current study was to test the reproducibility of different quantitative magnetic resonance imaging (MRI) methods to assess the morphologic and functional peripheral vascular status and vascular adaptations over time in patients with peripheral arterial disease (PAD).

Materials and methods: Ten patients with proven PAD (intermittent claudication) and arterial collateral formation within the upper leg and 10 healthy volunteers were included. All subjects underwent 2 identical MR examinations of the lower extremities on a clinical 1.5-T MR system, with a time interval of at least 3 days. The MR protocol consisted of 3D contrast-enhanced MR angiography to quantify the number of arteries and artery diameters of the upper leg, 2D cine MR phase contrast angiography flow measurements in the popliteal artery, dynamic contrast-enhanced (DCE) perfusion imaging to determine the influx constant and area under the curve, and dynamic blood oxygen level-dependent (BOLD) imaging in calf muscle to measure maximal relative T2* changes and time-to-peak. Data were analyzed by 2 independent MRI readers. Interscan and inter-reader reproducibility were determined as outcome measures and expressed as the coefficient of variation (CV).

Results: Quantification of the number of arteries, artery diameter, and blood flow proved highly reproducible in patients (CV = 2.6%, 4.5%, and 15.8% at interscan level and 9.0%, 8.2%, and 7.0% at interreader level, respectively). Reproducibility of DCE and BOLD MRI was poor in patients with a CV up to 50.9%.

Conclusions: Quantification of the morphologic vascular status by contrast-enhanced MR angiography, as well as phase contrast angiography MRI to assess macrovascular blood flow proved highly reproducible in both PAD patients and healthy volunteers and might therefore be helpful in studying the development of collateral arteries in PAD patients and in unraveling the mechanisms underlying this process. Functional assessment of the microvascular status using DCE and BOLD, MRI did not prove reproducible at 1.5 T and is therefore currently not suitable for (clinical) application in PAD.

Key Words: peripheral arterial disease, contrast-enhanced MRA, phase-contrast angiography, dynamic contrast-enhanced MRI, blood oxygen level-dependent

(*Invest Radiol* 2011;46: 11–24)

Peripheral arterial disease (PAD), characterized by atherosclerotic stenosis or occlusion of pelvic and/or lower extremity arteries, may manifest clinically as intermittent claudication or critical limb ischemia.[1] The primary treatment for patients with intermittent claudication is supervised exercise therapy, which may stimulate collateral blood artery formation to increase muscle perfusion.[1–3] Stimulation of collateral blood vessel growth is also the main target of angiogenic growth factor or stem cell administration to improve tissue oxygenation in patients with critical limb ischemia.[4–6] The exact mechanisms underlying this process are presently unknown, but are thought to involve both adaptation of existing arteries and the formation of new collateral arteries over time.[7] Furthermore, it is presently unknown to what extent different therapeutic options contribute to these vascular adaptive responses, and to what extent functional improvement of patients is related to such vascular adaptations.[1,8]

Uncertainties concerning the exact type and extent of vascular adaptations in humans are partly because of the lack of noninvasive diagnostic methods to visualize and quantify these processes. Quantitative noninvasive imaging tools that can be used to study the process of vascular adaptation and to monitor the effectiveness of vessel-stimulating therapies are therefore highly desirable. Magnetic resonance imaging (MRI) techniques are attractive for this purpose, as they provide high spatial resolution to visualize the entire peripheral vascular tree, including small collateral arteries. Furthermore, MRI techniques are suitable to obtain information on vascular morphology and function and allow repeated measurements without ionizing radiation exposure.[9–15] However, for evaluation of vascular responses over time, it is crucial that MRI provides reproducible quantitative measures.

The aim of the current study was to test the reproducibility of different MRI methods to assess the morphologic and functional vascular status and adaptations of the peripheral vasculature over time. Morphologically, the reproducibility was determined of a method to quantify the number of arteries in the upper leg, visualized by contrast-enhanced MR angiography (CE-MRA). Development of collateral arteries might result in an increased blood supply to and subsequent enlargement of the collateral re-entrance zone. This collateral re-entrance zone represents the level at which collaterals re-enter the large native conduit artery distal to an occluded segment of the arterial tree (distal superficial femoral or popliteal artery in our study), For this, the reproducibility of diameter measurements of the distal conduit artery was also assessed. Functional vascular status was determined both at macro- and microvascular level. Reproducibility of macrovascular function was studied by measuring peak arterial blood flow in the popliteal artery (PA) with quantitative 2D cine MR phase contrast angiography (PCA).[10,16–19] Reproducibility of microvascular function was determined in the calf musculature by perfusion measurements using dynamic contrast-enhanced (DCE) MRI[9,20,21] as well as the blood oxygenation measurements using dynamic blood oxygen level-dependent (BOLD) MRI.[13,22–27] All measurements were performed in a group of PAD patients with proven extensive collateral artery formation and a group of healthy volunteers.

MATERIALS AND METHODS

Phantom Study

A vessel phantom was used to determine the diameter of the smallest arteries that can be detected with our clinically used CE-MRA protocol. This phantom consisted of 10 tubes with varying inner diameters as follows: 6.00, 2.03, 1.57, 1.40, 1.01, 0.76, 0.51, 0.25, 0.18, and 0.13 mm. These tubes were filled with the same gadolinium-based contrast agent as used in the patient study (gadopentetate dimeglumine [Magnevist], Bayer HealthCare Pharmaceuticals, Berlin, Germany), with a concentration of 11 mmol/L, which is representative of the peak arterial concentration in our human study. Tubes were immersed in a muscle tissue mimicking fluid (T1 = 800 milliseconds, 0.2 mmol/L gadopentetate dimeglumine solution).

MRI was performed using the same acquisition protocol as used in the human studies detailed later in the text. Scan parameters are given in Table 1. Acquired voxel sizes were $1.22 \times 1.52 \times 2.4$ mm. Subsequently, voxels were interpolated to $0.92 \times 0.92 \times 1.2$ mm during reconstruction by zero-filling. The phantom was positioned slightly angulated with respect to the z-axis of the MRI scanner to average the signal over many subvoxel positions.

For image analysis, a line segment perpendicularly intersecting the depicted tubes was manually drawn. The intensity profile along this line was analyzed to determine the smallest detectable tube diameter by counting the number of peaks in the signal intensity profile.

Human Study

Over a period of 6 months, 10 patients (mean age, 64.7 ± 6.1 years; range, 57–73 years; 9 men and 1 woman) with proven PAD (intermittent claudication, Fontaine stage II, Rutherford stage 1–3) and arterial collateral vessel formation within the upper leg and 10 healthy volunteers without signs and symptoms of PAD (mean age, 26.7×11.5 years; range, 18–50 years; 2 men and 8 women) were included. PAD patients were eligible for the study if peripheral CE-MRA examinations as part of routine diagnostic work-up confirmed the presence of superficial femoral artery (SFA) occlusion with a collateral arterial network in the upper leg. Patients with contraindications to MRA, including claustrophobia, known gado-

linium-based contrast-agent allergy, and low estimated glomerular filtration rate (<30 mL/kg/1.73 m^2) were excluded from participation. The study was approved by the institutional medical ethics committee and all patients and healthy controls gave written informed consent before inclusion.

Magnetic Resonance Imaging

All subjects underwent 2 MRI examinations on different days (mean interval, 14.6 days; range, 3–68 days). An overview of the imaging protocol is given in Figure 1. The entire examination lasted 1 hour. Patients received no treatment between both examinations. All examinations were performed on a 1.5-T commercially available system (Intera, Philips Medical Systems, Best, The Netherlands). For signal reception, we used a dedicated 12-element phased-array peripheral vascular coil with craniocaudal coverage of 128 cm (Philips Medical Systems, Best, The Netherlands). Subjects were imaged in the supine position and care was taken not to deform calf muscle by calf-bed contact. All subjects were lying in this position for at least 15 minutes before the first measurement was started. Scan parameters for all acquisitions are given in Table 1.

Contrast

For CE-MRA and DCE MRI, a dose of gadopentetate dimeglumine respectively 30 and 15 mL (Magnevist, Bayer HealthCare Pharmaceuticals, Berlin, Germany) was injected intravenously as a single biphasic bolus in the cubital vein, using a remote-controlled injection system (Medrad Spectris, Indianola, PA). Although CE-MRA for this study comprised only 1 station (upper leg), an injection of 30 mL of contrast agent was chosen for best comparison of image quality with common clinical 3-station peripheral CE-MRA, for which we normally administer a single bolus of 30 mL. After contrast medium administration, 20 mL of saline was injected. Real-time bolus monitoring software (BolusTrak, Philips Medical Systems, Best, The Netherlands) was used to visualize the arrival of the bolus in the proximal SFA with a refresh rate of proximally 1 frame/s. Upon first sight of contrast arrival in the proximal SFA, image acquisition for the CE-MRA sequence was started. For DCE MRI, cuff inflation (mentioned later in the text) was immediately

TABLE 1. Acquisition Parameters for All MRI Measurements

Parameter	MR Measurement				
	TOF	**CE-MRA**	**PCA**	**DCE**	**BOLD**
Scan mode	Multi2D	3D	2D	3D	MS
Technique	TFE	FFE	FFE	FFE	FFE
TR (ms)	11.0	4.8	7.9	8.0	1000
TE (ms)	6.9	1.45	4.7	0.91	30
Flip angle (deg)	50	40	30	30	90
FOV (mm)	450	470	320	400	300
Voxel dimensions (acquired) (mm)	$1.76 \times 1.76 \times 3.3$	$1.22 \times 1.52 \times 2.4$	$1.25 \times 1.67 \times 6.00$	$3.13 \times 3.13 \times 12.0$	$3.13 \times 3.26 \times 2.5$
Voxel dimensions (reconstructed) (mm)	$1.76 \times 1.76 \times 3.3$	$0.92 \times 0.92 \times 1.2$	$1.25 \times 1.25 \times 6.00$	$3.13 \times 3.13 \times 6.0$	$3.13 \times 3.13 \times 2.5$
No. slices	31	100–160*	1	12	4
Scan direction	Transversal	Coronal	Transversal	Transversal	Transversal
Parallel imaging acceleration (Factor/direction)	No	Yes (2/R-L)	No	Yes (2/R-L)	No
Dynamic scans	—	—	—	80	400
Dynamic scan time (s)	—	—	—	2.6	2.0
Total scan duration(min:s)	1:34	0:25–0:43*	2:16†	3:31	13:23

*For CE-MRA the number of slices, and therefore scan duration, varied from subject to subject, depending on the dimensions of the upper leg.
†Nominal scan duration at a heart rate of 60 beats per minute.
MR indicates magnetic resonance; CE-MRA, contrast-enhanced MR angiography; PCA, phase contrast angiography; DCE, dynamic contrast-enhanced; BOLD, blood oxygen level-dependent; MS, multislice; TFE, turbo field echo; FFE, fast field echo (gradient echo); FOV, field of view.
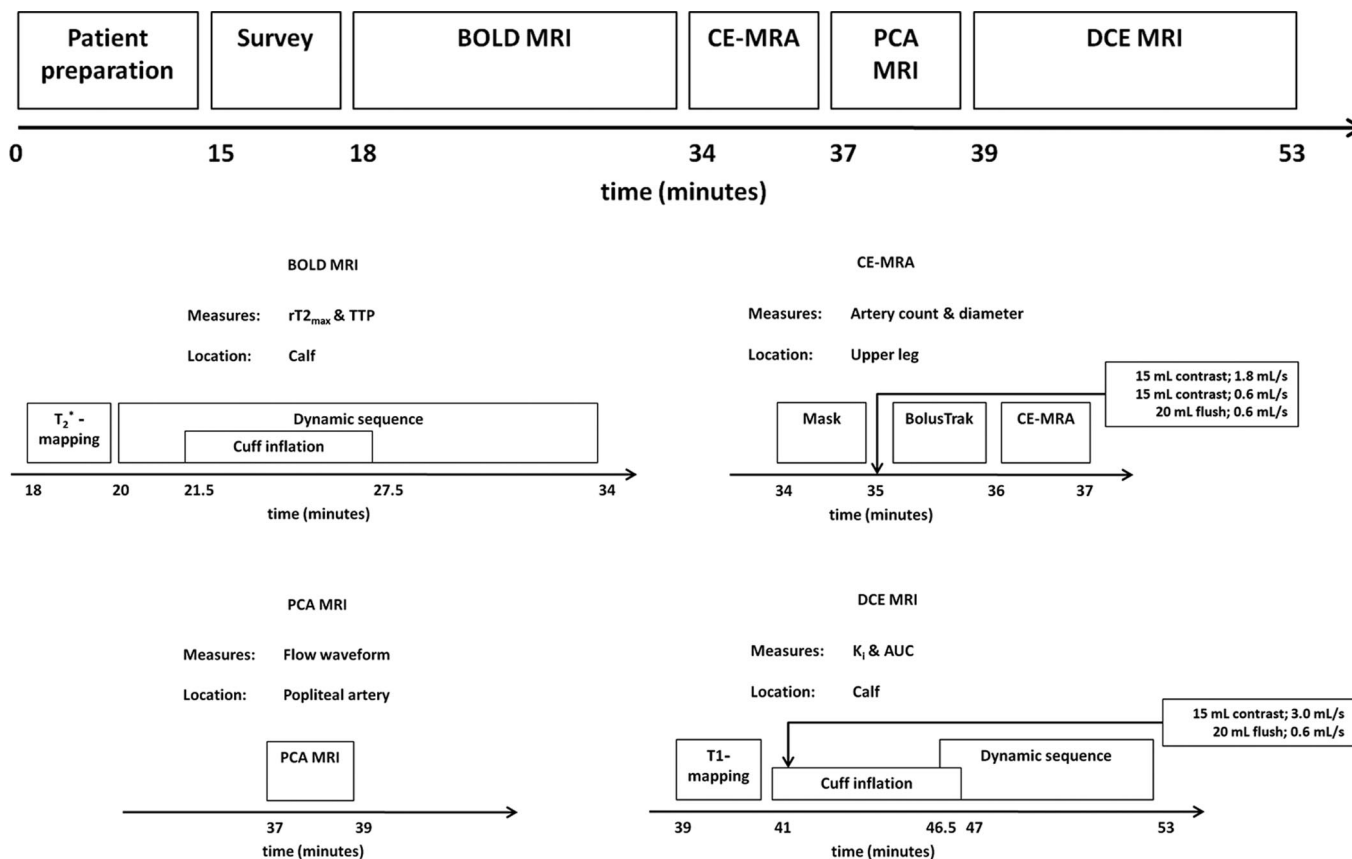
FIGURE 1. Overview of imaging protocol, approximate duration of each scan, and the obtained quantitative measures. Contrast-enhanced MR angiography (CE-MRA) was combined with phase-contrast angiography (PCA) flow MRI, dynamic contrast-enhanced (DCE) MRI, and blood oxygen level dependent (BOLD) MRI. The BOLD measurement was performed prior to contrast agent administration, as needed for the CE-MRA and DCE perfusion measurement. Total MRI examination, including patient positioning, table movements, and MRI scans, took 1 hour.

followed by a single bolus of 15 mL contrast agent, allowing systemic contrast equilibration in the arterial blood pool proximal to the occlusion during cuff compression.

Cuff Paradigm

For DCE and BOLD MRI, postischemic reactive hyperemia was provoked in both lower legs using inflatable cuffs (Medrad, Indianola, PA). Reactive hyperemia was provoked to ensure measurable signal alterations in DCE and BOLD MRI and to ensure a most reproducible state of vasodilatation for both examinations for each patient.[13] A cuff paradigm was chosen, as this method was believed to be more reproducible and suitable for MRI in comparison with muscle exercise and less invasive in comparison with drug-induced vasodilation. Besides, a cuff paradigm ensures a vascular step-input function of contrast agent, as preferred for DCE MRI.[9] The cuffs were placed at midthigh level and manually inflated to suprasystolic values (>50 mm Hg above brachial systolic blood pressure) during 6 minutes prior to BOLD and DCE MRI, ensuring total arterial occlusion.[13]

Survey

A nonenhanced time-of-flight (TOF) scan of the pelvic, upper and lower leg station was acquired to prescribe the imaging volumes of interest for morphologic and functional imaging. A turbo field echo pulse sequence was used with a 180° inversion prepulse to suppress stationary tissues. Thirty-one axial slices per station were

acquired with 3.3-mm slice thickness and 11-mm interslice gap, and an inferiorly concatenated saturation band. The standard quadrature body coil was used for signal transmission and reception. For positioning of the 3D CE-MRA volumes, maximum intensity projections were generated in 3 orthogonal directions.

Contrast-Enhanced MR Angiography

An 1-station, 3D CE-MRA was performed with voxel sizes identical of the phantom study. Although clinical CE-MRA examinations are usually limited to visualization of a thin antero-posterior imaging volume only including the large conduit arteries in the upper leg (ie, SFA and PA), for this study, the entire muscular volume of the upper leg was imaged to visualize all the arteries including any collateral branches within the upper leg. Prior to contrast medium administration, a nonenhanced "mask" image data set was acquired with exactly the same acquisition parameters as the CE-MRA, enabling background tissue suppression by image subtraction.

Phase Contrast Angiography MRI

Blood flow data were obtained in the PA (distal to the vascular lesion in the SFA in patients). A single slice was positioned perpendicular to the course of the PA. In all, 20 cardiac phases were acquired over the R-R interval with an encoding velocity (venc) of 100 cm/s in the craniocaudal direction. Vector CardioGraphy tracing

was used for retrospective cardiac synchronization. The nominal duration of this acquisition was 136 seconds at a heart rate of 60 beats per minute.

Dynamic Contrast-Enhanced MRI

DCE-MRI was preceded by T1 mapping to determine precontrast T1 relaxation times before contrast enhancement, using a scan sequence with identical contrast parameters and geometry as for the subsequent DCE acquisitions, but with variable flip angles (2°, 5°, 10°, 15°, 25°, and 35°).[9,28] A dynamic 3D T1-weighted gradient echo sequence was used for DCE MRI (Table 1). Slices were positioned at the maximum diameter of the calf. Five dummy scans were acquired before the actual measurement to avoid varying T1 saturation effects. The acquisition started 330 seconds after cuff inflation. The cuff was then rapidly deflated (within 2 seconds) together with the start of the sixth dynamic scan.

Blood Oxygen Level-Dependent MRI

For BOLD imaging, a multishot single-echo echo planar imaging sequence with fat suppression (spectral presaturation with inversion recovery) was used to detect the T2* responses to oxyhemoglobin changes. Slices were also positioned at the maximum diameter of the calf. The first 1:30 minutes of the measurement were used to obtain baseline values. The cuff was then inflated for 6 minutes, while the measurement continued (data not used for analysis) and after cuff deflation, the measurement continued for approximately 6 minutes. The dynamic study was preceded by a series of echo planar imaging sequences to determine the T2* relaxation time of muscle tissue, using the same parameters and geometry but increasing echo times of 10, 15, 20, 30, 40, and 50 milliseconds.

Image Analysis

In patients the most symptomatic leg was analyzed for all measurements. In healthy volunteers, reproducibility measures were determined for both legs separately and these measures were subsequently averaged. Two independent MRI readers (M.E. and B.V.) analyzed all data sets, blinded for each other's results and the order of the examinations.

Vascular Morphology

Contrast-Enhanced MR Angiography

Image analysis was performed on a dedicated image postprocessing workstation (MacPro, running OS X, version 10.5.4, Apple Inc., Cupertino, CA). Both source images and subtracted images were analyzed to ensure that no collateral arteries were missed due to misregistration artifacts between the source and mask images.

The MRI readers manually quantified the number of collaterals by counting the total number of arteries crossing transverse planes in the upper leg at 5 different levels. In patients, arteries were counted at the following levels: 5 cm below, exactly at, and 5, 10, and 15 cm above the location where the SFA was reconstituted distal to the occlusion (Fig. 2). In volunteers, these planes were located at 10, 15, 20, 25, and 30 cm above the distal margin of the femoral condyles, as this corresponded best to the levels used in patients. In volunteers, both legs were analyzed, whereas in patients only the most symptomatic leg (ie, with clinically significant vascular pathology) was analyzed.

Arteries were counted using the open source DICOM viewer OsiriX (OsiriX, Geneva, Switzerland, version 3.5.1, http://www.osirix-viewer.com/), using the original source images as well as coronal and sagittal multiplanar reconstructions. Identification of the correct counting plane was ensured by placing a crosshair at the anatomic landmarks as described earlier in the text. Subsequently, the total number of arteries intersecting the 5 planes was
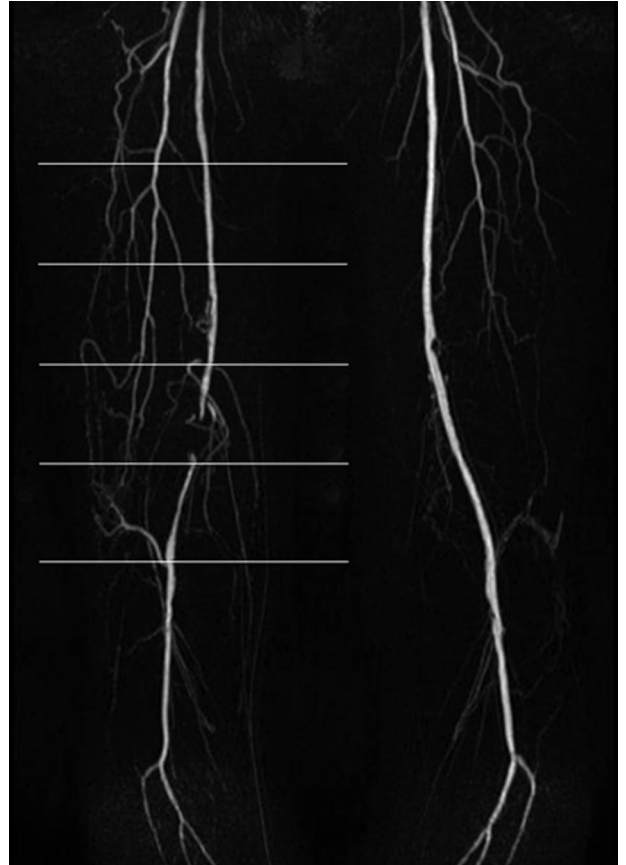
FIGURE 2. Maximum intensity projection (MIP) after background subtraction of a CE-MRA in a PAD patient with segmental occlusion of the superficial femoral artery with extensive collateral blood vessel formation. The image shows the location of the 5 transverse planes, represented by the 5 horizontal lines, at which quantification of the number of arteries was manually performed. This MIP image is used to demonstrate the locations of the measurements; the actual measurements were performed using the 3D image data set.

determined, including conduit arteries (SFA or PA), terminal muscle branches, and any collateral arteries. Arteries were distinguished from veins by scrolling through source images and multiplanar reconstructions stacks when it was necessary to find an upstream connection to a named artery.

Diameter of the collateral re-entrance zone and image quality, in terms of contrast-to-noise ratio (CNR), was assessed on source images. Artery diameter and CNR were determined below the vascular lesion at the level of the collateral re-entrance zone (distal SFA or proximal PA in PAD patients or at the level of the PA in healthy volunteers). Artery diameter was measured at the coronal source images by manually drawing a line segment perpendicular to the artery at the same location as the most inferior transverse plane, used for counting the arteries. Next, the intensity profile along this line was obtained to determine the full width at half maximum of the arterial lumen, which represented the arterial diameter. Image quality of vascular depiction was expressed as the CNR, which was defined as the difference between signal intensity within the vessel and a similarly sized region of interest (ROI) directly adjacent to the vessel.

Vascular Function

Phase Contrast Angiography MRI

Modulus and phase images were reconstructed from the PCA data. The image software application MRIcro (MRIcro, http://www.mricro.com/) was used to manually draw a ROI covering the entire visible surface of the PA on each of the 20 reconstructed modulus images spanning the R-R interval. These ROI's were analyzed, using self-written software code (Matlab, The Mathworks Inc., Natick, MA) to obtain velocity and flow waveforms from the phase images. Reproducibility was determined for the peak flow (unit: mL/s), as flow has been shown to be a more reliable parameter compared with velocity and peak values have shown larger differences between patients and healthy volunteers and proven to be more reliable compared with mean values for small arteries like the PA.[10]

Dynamic Contrast-Enhanced MRI

MRIcro was used to manually draw large ROI's covering the entire cross-section of the calf muscle (including vessels) in 4 successive slices. Special attention was given to draw ROI's of both scans for every subject at the same location.

Self-written Matlab software code was used for the analysis of T_1-weighted signal intensity time courses for each ROI. Individual signal time courses were normalized with respect to resting values, measured prior to contrast agent arrival, and converted to contrast agent concentration, using the relation between T_1 relaxation time and the signal intensity for a spoiled gradient echo pulse sequence. Signal to contrast agent concentration conversion was applied to correct for the presence of residual contrast agent from the CE-MRA, which may vary between patients and healthy volunteers. In addition, contrast concentration is less scan technique dependent compared with signal intensity.

A vascular input function (VIF) could not be obtained in every patient. Therefore, a predefined step-wise VIF with a maximum (ie, step size) concentration of 0.45 mM was used for data analysis.[9] The influx constant (K_i, unit: $\min^{-1}$) and area under the curve (AUC, unit: mMs) up to 90 seconds after contrast arrival were calculated as surrogate markers of microvascular blood flow.[9] Reproducibility was determined for both K_i and AUC.

Blood Oxygen Level-Dependent MRI

Analogous to DCE MRI, a large ROI, covering the entire cross-section of the calf muscle was drawn in the 4 acquired slices to assess skeletal muscle oxygenation. Self-developed Matlab software code was used for analysis of the T2* signal intensity time courses for each of the ROI's. Individual T2* time courses were divided by the average T2* values measured prior to cuff inflation. The maximum relative T_2* change after cuff deflation relative to the resting condition value (rT2$_{max}$, unit: %) and time-to-peak (TTP) (unit: s) were determined.[13] rT2$_{max}$ and TTP were both used to determine the reproducibility of the BOLD technique.

Statistical Analysis

To determine reproducibility, 2 agreement measures, being the coefficient of variation (CV in %) and the repeatability coefficient (RC), and a measure for reliability, the intraclass correlation coefficient (ICC) were determined. The CV is derived by dividing the overall mean within-subject standard deviation (SD$_{ws}$) by the mean measurement value over all subjects. The RC gives the smallest noticeable difference that can be detected beyond measurement error and is defined as $1.96 \cdot \sqrt{2} \cdot SD_{ws}$.[29,30] The difference between 2 measurements in the same subject is expected to be less than the RC in 95% of the observations in cases where the measured quantity remains unchanged over time. A value of RC (or CV) lower than absolute (or relative) difference between mean values in patients and controls indicates good agreement. The ICC was calculated using a 1-way random model, according to ICC = $SD_{bs}^2/(SD_{bs}^2 + SD_{ws}^2)$, where SD$_{bs}$ represents the SD between subjects. The ICC is the fraction of total variance because of variation between subjects, rather than measurement error, and ranges between 0 and 1. If the measurement error is small compared with the variation between subjects, the ICC approaches 1, ie, reliability is very high.

Figure 3 schematically illustrates how interscan and interreader reproducibility were defined. Interscan reproducibility is influenced by contrast injection, vascular opacification, positioning
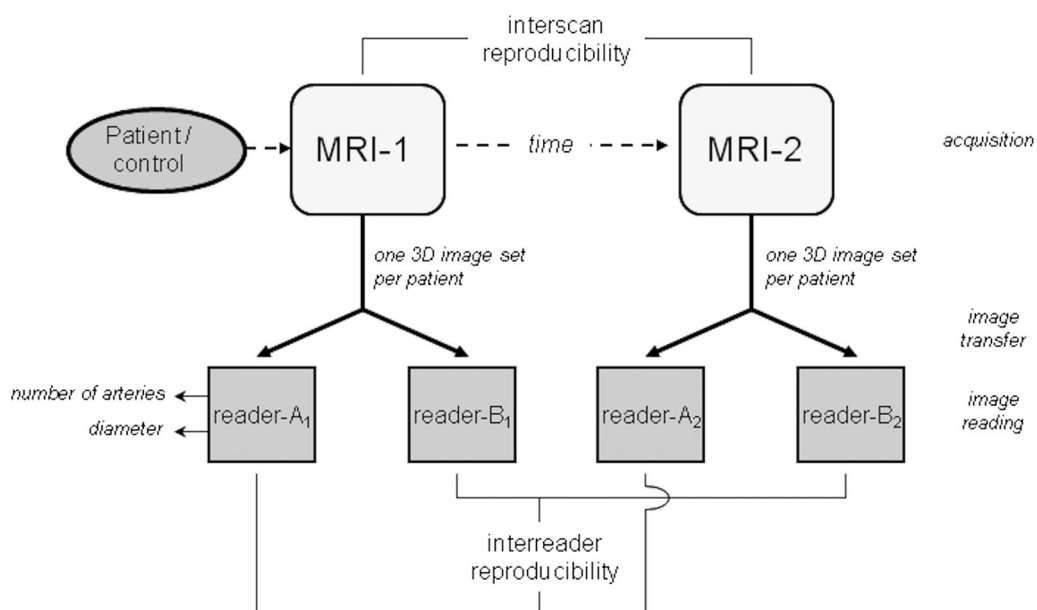

**FIGURE 3.** Schematic overview to define the interscan and interreader reproducibility.

of the patient within the coil or magnet, preparation of the patient, physiological variances within the patient, and reader errors. Interscan reproducibility is mainly influenced by scan-related inconsistencies and was calculated by averaging the results of both MRI readers for each scan (mean of MRI 1 for reader A and B vs. the mean of MRI 2 for reader A and B in Fig. 3). Inter-reader reproducibility is an indicator of image reading error and is primarily influenced by reader experience. Inter-reader reproducibility was calculated by averaging the results of both scans for each MRI reader (mean of reader A for MRI 1 and MRI 2 vs. the mean of reader B for MRI 1 and MRI 2 in Fig. 3).

Secondary to the reproducibility, an independent samples *t* test was performed to test the significance of differences in parameters between patients and healthy volunteers. $P < 0.05$ was considered statistically significant. All statistical analyses were performed with commercially available statistical software (SPSS 16.0, SPSS Inc., Chicago, IL).

RESULTS

Vessel Phantom

Figure 4 displays a thin-slab maximum intensity projection image of the vessel phantom. The smallest tube visualized had a

0.51 - 0.76 - 1.01 - 1.40 - 1.57 - 2.03 mm
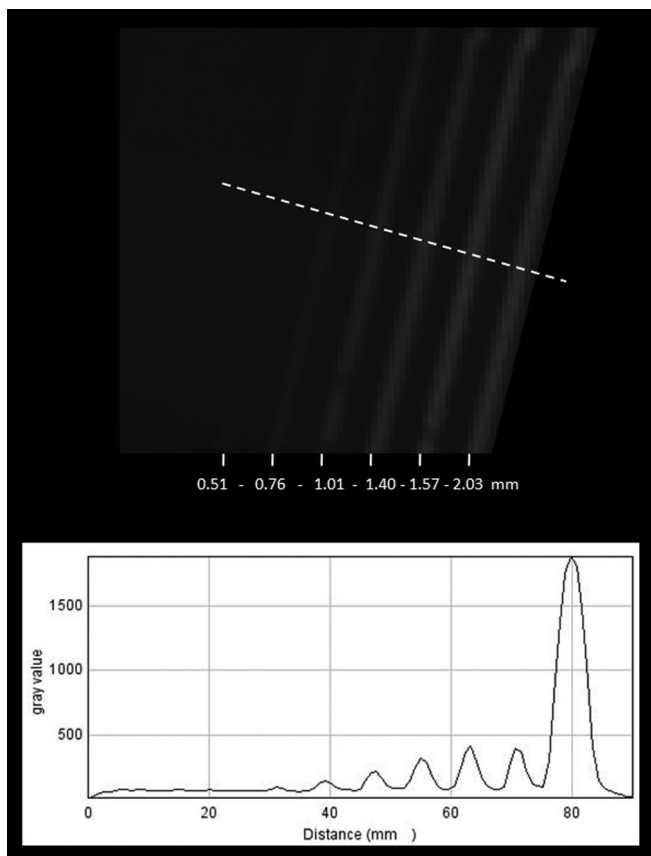
FIGURE 4. Thin slab (5 slices) maximum intensity projection (MIP) image showing the tubes with various diameters. Of 10 tubes, 7 can be distinguished. Graph shows the signal intensity profile measured at the level of the dotted line in the MIP image. The 6-mm tube with the highest signal intensity has been removed from the image to improve contrast.

diameter of 0.51 mm. The smallest peak visible in the signal intensity profile matched the smallest tube visible on the MR angiogram.

Subjects

All patients and healthy volunteers underwent both MRI examinations without experiencing side effects or adverse events. In 1 patient, there were severe subtraction misregistration artifacts in CE-MRA due to the patient movement between acquisition of the mask and the contrast-enhanced data sets. For this patient, only the original contrast-enhanced images were analyzed. Reactive hyperemia could not be provoked in 2 out of 10 patients as the cuff broke during cuff inflation. There were no side effects or adverse events in any of the study subjects. Severe discomfort due to cuff inflation was reported in 3 out of the 8 patients and 3 out of the 10 volunteers.

Vascular Morphology

Artery Count

Table 2 lists the number of arteries and reproducibility measures for source and subtracted images in patients and volunteers. Interscan and interreader reproducibility were better for source images compared with subtracted images for both groups. Furthermore, RC at interscan level was roughly 4 times lower than the RC at interreader level, indicating better agreement at interscan level. There were no relevant differences in reproducibility measures between patients and volunteers, both at interscan and interreader levels. In Figure 5, Bland-Altman plots are shown for artery count on CE-MRA source images for interscan and interreader variations.[31] Both for patients and volunteers, the range between the 95% limits of agreement is much narrower, and therefore better, at interscan level compared with inter-reader level.

No significant differences were found in mean number of arteries per plane between the source and subtracted images in both patients and volunteers. The number of arteries per plane was significantly higher in patients compared with volunteers for CE-MRA ($P < 0.05$).

Artery Diameter

In Table 3, results of the arterial diameters of the collateral re-entrance zone in patients and PA in volunteers are listed. Analogous to the artery count, the interscan RC in patients was better than inter-reader RC, whereas in volunteers the reverse was found. This was the case true for the CV in patients and volunteers. ICC was low in volunteers with respect to interscan level reproducibility. In Figure 6, Bland-Altman plots are shown for the collateral re-entrance zone on source images at interscan and interreader level for both patients and healthy volunteers.[31] The 95% limits of agreement show no large differences between interscan and interreader diameters for both patients as well as volunteers.

No significant differences were found in artery diameters between patients and volunteers ($P = 0.43$).

Image Quality

CNR values of the CE-MRA images are also listed in Table 3. Patients showed a significantly lower CNR compared with volunteers ($P < 0.05$).

Vascular Function

Phase Contrast Angiography MRI

Examples of measured waveforms are shown in Figure 7. In Table 4, the results of the reproducibility of the flow assessment are listed. In general, reproducibility of peak flow was good according to all different measures of agreement and reliability, with an interscan CV in patients up to 15.8%. Interreader reproducibility

TABLE 2. No. Arteries per Plane and Reproducibility of Artery Count

	Patients		Volunteers	
	Source Images (n = 10)	Subtracted Images (n = 9)	Source Images (n = 10)	Subtracted Images (n = 10)
Arteries per plane	15.7 ± 3.5	14.5 ± 3.2*	12.9 ± 2.5	13.1 ± 2.3[†]
Interscan reproducibility				
CV (%)	2.6	6.1	2.8	3.1
RC	1.1	2.5	1.0	1.1
ICC (95% CI)	0.99 (0.95–0.99)	0.92 (0.75–0.98)	0.98 (0.90–0.99)	0.97 (0.89–0.99)
Interreader reproducibility				
CV (%)	9.0	10.1	11.1	10.0
RC	3.9	4.1	3.9	4.5
ICC (95% CI)	0.85 (0.56–0.96)	0.81 (0.44–0.95)	0.73 (0.12–0.95)	0.74 (0.18–0.94)

Number of arteries is expressed as mean ± SD.
*$P = 0.19$.
[†]$P = 0.43$.
CV indicates coefficient of variance; RC, repeatability coefficient; ICC, intraclass correlation coefficient; 95% CI, 95% confidence interval; SD, standard deviation.

was better than the interscan reproducibility, especially for the patient group.

Flow waveforms in patients were either bi- (n = 3) or monophasic (n = 7), whereas triphasic flow waveforms were obtained in all volunteers (Fig. 7). The peak flow in the PA of patients was less than 1/3 compared with peak flow of healthy volunteers ($P < 0.01$). For PCA MRI, there was no relevant difference in any of the reproducibility measures between patients and healthy volunteers.

Dynamic Contrast-Enhanced MRI

Examples of DCE MRI-derived time courses are shown in Figure 8. DCE-MRI interscan reproducibility was poor in patients for both Ki and AUC with interscan CV values up to 51% (Table 5). Interreader reproducibility, on the contrary, was good with a low CV and RC, indicating a strong agreement between the readers, and a high ICC, indicating good interreader reliability. Interreader reproducibility was comparable between patients and healthy volunteers.

Ki of the entire cross-section muscular volume showed a trend of lower perfusion values in the calf of patients compared with healthy volunteers ($P = 0.07$), whereas the AUC showed a trend of higher values in patients ($P = 0.09$).

Blood Oxygen Level-Dependent MRI

Examples of BOLD time courses are shown in Figure 9. In patients, BOLD-derived parameters had interscan CV values in $rT2_{max}$ and TTP of up to 27% and 11% respectively and these results were comparable with those found in healthy volunteers (Table 6). The interreader reproducibility was better in patients for both BOLD parameters and had CV values of up to 1.5% for rT2max and 11.3% for TTP (Table 6).

TTP was delayed ($P < 0.01$) in the patient group compared with the volunteers, whereas the rT2max was nearly equal ($P = 0.97$).

DISCUSSION

The reproducibility of morphologic and functional MRI techniques able to assess the vascular status in patients with PAD and healthy volunteers was evaluated. At morphologic level, we presented an easy and reproducible method to quantify the number of arteries with a detection limit of 0.5 mm and a method to assess the diameter of the collateral re-entrance zone in the upper leg. For vascular function, we investigated the reproducibility of 3 different MRI techniques to assess macrovascular PA blood flow and microvascular calf muscle perfusion and blood oxygenation. Measurement of peak arterial flow in the PA proved reproducible, whereas all DCE MRI-derived parameters and the $rT2_{max}$ parameter for BOLD MRI in the lower leg are poorly reproducible in PAD patients. TTP in BOLD MRI was identified as a fairly reproducible microvascular parameter.

Objective assessment of the hemodynamic consequences of stenoses and occlusions in the peripheral arterial tree remains an area of high interest in the diagnostic workup and treatment of patients with PAD. A simple and cost-effective way to assess the functional severity of PAD is the ankle-brachial index, which is the ratio of the systolic blood pressures measured at the level of the ankle and the upper arm.[32] However, the ankle-brachial index is a relatively crude parameter as it is not able to pinpoint the exact location of a stenosis, is unreliable in patients with an uncompressible vessel wall due to arterial calcifications, and shows a large interobserver variability.[33]

Other known techniques to determine vascular function are Doppler-based flow measurements, plethysmography, skin perfusion pressure measurements, positron emission tomography (PET), contrast-enhanced ultrasound (CEUS), and intra-arterial pressure and/or flow measurements.[34–43] Unfortunately, these methods either lack the spatial resolution or coverage to directly measure the effect of vascular adaptations (eg, collateral vessel formation or changes in microcirculation), or are unfavorable for repeated measurements for instance in the context of therapy monitoring due to invasiveness, use of ionizing radiation, or large interobserver variability.[33] MRI has the potential to overcome these limitations and can facilitate a variety of functional measurements at both the macro- and microvascular level. In particular, MRI may enable comprehensive diagnostic imaging of both the anatomy of the peripheral vascular tree as well as vascular function in terms of macrovascular flow and surrogate parameters of tissue perfusion and oxygenation.[9,10,13,21,25,44,45] MRI-based functional measurements have the advantage that they can be applied repeatedly without detrimental side effects and are easy to add to clinical routine CE-MRA examinations.

We sought to investigate whether MRI can be used to combine its well-known high-quality depiction of peripheral vascular anatomy with noninvasive assessment of macrovascular and microvascular hemodynamics.[12] Combined assessment of vascular morphology and function using 1 noninvasive accurate MRI examination is of high clinical interest for the diagnostic workup as well as
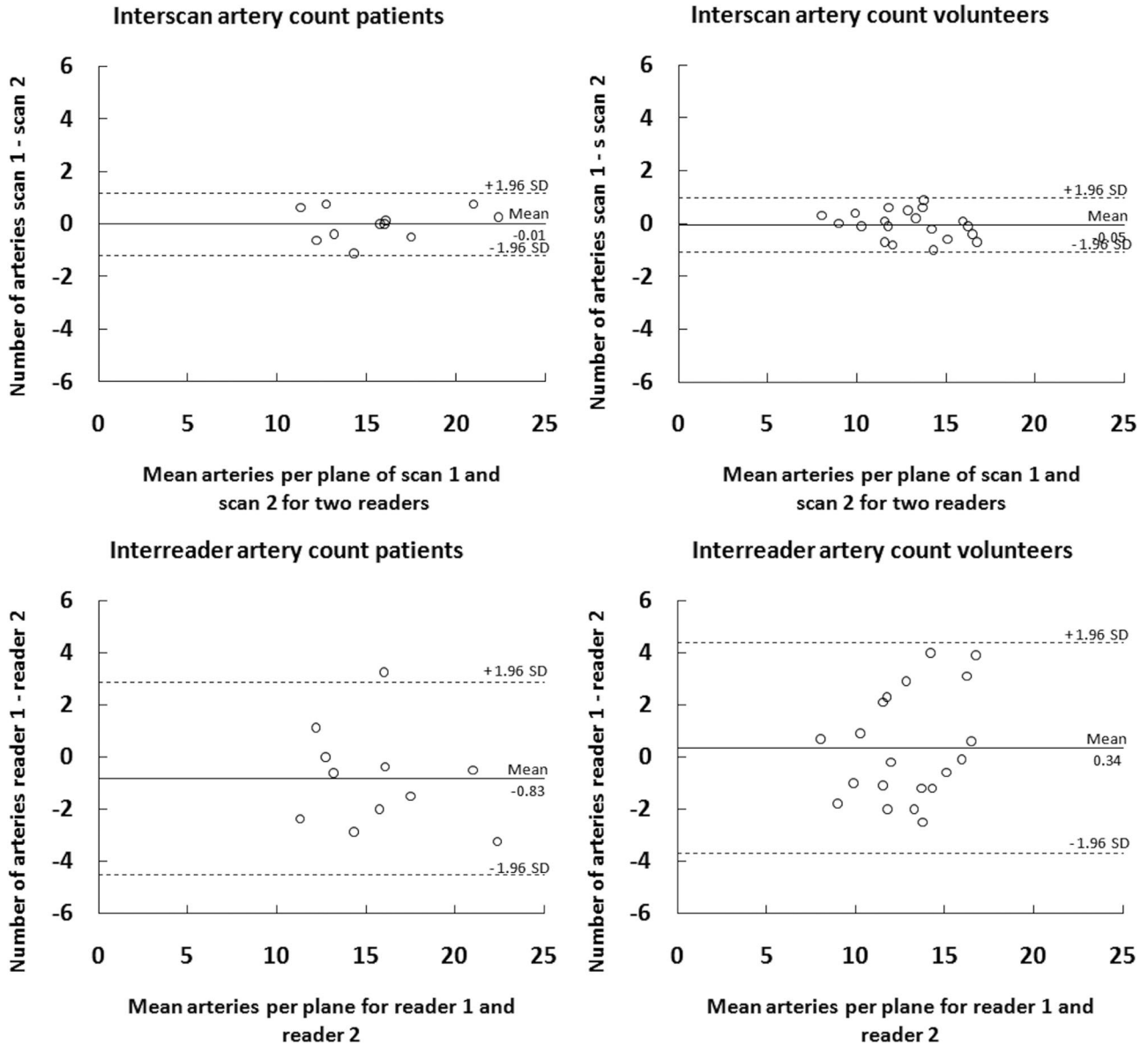
FIGURE 5. Interscan and interreader reproducibility of number of arteries per plane in PAD patients and volunteers. Bland-Altman plots showing difference in number of arteries between scans (interscan) or readers (interreader) (y-axis) against mean number of arteries (x-axis). Absolute mean difference is represented by the solid line and 95% confidence interval is given by the 2 dashed lines.

for monitoring the effects of novel therapeutic strategies in patients with PAD. Although all of the MRI techniques as applied in this study have been described previously,[9–11,13] little is known about the reproducibility of flow, perfusion, and oxygenation-sensitive MRI in the lower extremity. To our knowledge, this is the first study on interscan and interreader reproducibility of quantitative MRI-derived morphologic and functional measures in the context of PAD.

Vascular Morphology

Artery Count

Interscan reproducibility for the artery count, as expressed by various measures of agreement and reliability, was high in both patients and healthy volunteers. The RC indicates the smallest noticeable increase in the number of visualized arteries that can be

confidently determined by the current combination of image acquisition and analysis methods. Lower RC values signify the capability to detect smaller differences in (longitudinal) follow-up studies. In both patients and volunteers, the interscan RC was approximately 1 artery per plane, meaning that a mean increase of 1 or more artery per plane obtained at 2 different time points can be detected beyond measurement error. In other words, any additionally formed or sufficiently matured artery, exceeding a diameter of 0.5 mm, will be detectable during treatment monitoring in PAD patients, using the sequence parameters as described earlier in the text.

The RC at interreader level was roughly 4 times as high as the RC at interscan level. This indicates that when different readers are used and an increase in less than 4 collateral arteries is detected, it cannot be concluded with certainty that this increase represents a

TABLE 3. Artery Diameter, Reproducibility, and Contrast-to-Noise Ratio

	Patients (n = 10)	Volunteers (n = 10)
Arterial diameter (mm)	6.9 ± 1.2	7.0 ± 0.7*
Interscan reproducibility		
CV (%)	4.5	5.6
RC (mm)	0.8	1.1
ICC (95% CI)	0.94 (0.79–0.98)	0.71 (0.39–0.88)
Interreader reproducibility		
CV (%)	8.2	4.0
RC (mm)	1.5	0.8
ICC (95% CI)	0.79 (0.44–0.94)	0.84 (0.63–0.94)
CNR	64 ± 31	84 ± 31[†]

Arterial diameter is expressed as mean ± SD.
*$P = 0.43$.
[†]$P < 0.05$.
CV indicates coefficient of variance; RC, repeatability coefficient; ICC, intraclass correlation coefficient; 95% CI, 95% confidence interval; CNR, contrast-to-noise ratio; SD, standard deviation.

real change. This larger RC at interreader level is probably the result of differences in experience of the MRI readers and in reading conditions. Given the larger RC at interreader level, it would be advisable to use the same observer at different points in time. This is not a surprising finding as advanced postprocessing techniques are often dependent on the experience of the observer performing the measurements, as has also been demonstrated for abdominal aortic neck volumetry and diameter assessment, which shows good intraobserver, but poor interobserver reliability.[46]

The interreader ICC was evidently lower in healthy volunteers compared with patients. A low ICC is unfavorable, as it compromises reproducibility. However, the lower ICC for healthy volunteers can be explained by the fact that these volunteers represent a more homogenous group of subjects, with lower SD_{bs} (Table 2), as opposed to patients harboring a wider range of vascular pathology. Because of this lower SD_{bs} and comparable SD_{ws} for patients and volunteers, the SD_{ws} has more influence on the ICC and the proportion of total variance that is explained by SD_{bs} is smaller. A significantly higher number of arteries per plane were found in patients with PAD compared with healthy volunteers. This was to be expected, as patients were selected for this study based on the presence of collateral arteries. Volunteers did not suffer from PAD and did not have an extensive collateral network. Instead, only the terminal muscular branches of the deep femoral artery were counted. In this study, we therefore studied the 2 extremes of the possible spectrum of disease that may be encountered in clinical practice: a pathologic vascular system with diseased conduit arteries, muscular branches and extensive collateralization versus a healthy vascular tree with patent conduit arteries and muscular branches but lacking collateral arteries. For determination of reproducibility of artery count, which was the primary aim of this study, these differences appeared to be of only minimal influence, indicating the robustness of this method.

Artery Diameter

Interscan reproducibility was reasonable for diameter assessment in patients and volunteers, with an average RC of approximately 1 mm. A better RC would not have been realistic given the voxel sizes used in the imaging protocol. Interreader reproducibility in patients was less favorable than interscan reproducibility, as was the case for the artery count. Therefore, in patients, for follow-up

studies the same image reader for 1 patient is advised. Nevertheless, in absolute terms, the differences between interscan and interreader reproducibility were very small. In patients, the RC at both interscan and interreader levels differed only by 0.7 mm, which is actually lower than the resolution of the images. In volunteers, interreader reproducibility was equal to or slightly better than interscan reproducibility. This can be explained by the fact that the physiological variance in volunteers with healthy arteries (which influences interscan reproducibility) is somewhat higher than the interreader variance.

Given the good reproducibility and especially the low RC values, diameter assessment of the collateral re-entrance zone may help to study morphologic changes due to collateral formation, as we expect an increase in diameter over time of this re-entrance zone when collateral arteries are developing and blood supply distal to a high-grade stenosis or occlusion improves.

In this study, we did not find a significant difference in artery diameter between patients and volunteers, although a smaller diameter in patients might have been expected. This finding may be explained by a difference in location at which the diameter was assessed between subjects. In volunteers, the measurement was always performed 10 cm above the distal margin of the femoral condyles, whereas in patients, the assessment was performed 5 cm distal to the vascular lesion (in most cases the PA), resulting in a large variance. More importantly, however, is the fact that we only included patients with already well-developed collateral arteries, which reconstituted the main conduit artery distal to the occlusion to a near-normal diameter.

Image Quality

All examinations were of sufficient quality for analysis, with the exception of 1 subtracted image stack in a PAD patient. A lower CNR in patients is most likely inherent to the presence of PAD, as impaired flow because of vascular lesions will result in lower signal intensity in the vessels distal to vascular lesions. In addition, for patients it is often harder to lie perfectly still during the examination, which results in increased noise levels due to subtraction misregistration.

Source Versus Subtracted Images

An important insight from this study is the finding that image subtraction leads to a deterioration of the reproducibility of the artery count compared with the detection of small arteries on source images. This is surprising because image subtraction leads to better background suppression and better visualization of small vascular structures,[47] and is therefore widely applied in clinical practice. A possible explanation for this finding is that small subtraction misregistration errors as well as the well-known $\sqrt{2}$ increase in image noise after subtraction apparently do not disturb qualitative evaluation of peripheral MR angiograms for purposes of stenosis detection, but do influence quantitative assessment of the number of arteries as well as arterial diameter.

Vascular Function

Phase Contrast Angiography MRI

We found favorable values for the interscan and interreader reproducibility measures for the peak arterial flow in the PA in both patients and healthy volunteers, indicating good reproducibility of PCA MRI over a broad range of flow conditions. Although the interscan CV in patients run up to 15.8%, both CV and RC were clearly lower than the relative and absolute differences in peak flow between PAD patients and healthy volunteers, making the PCA derived peak flow perfectly suitable for a reliable, objective gauge of PAD severity and therapy monitoring. Minor variations in interscan results are probably the result of biologic variation in PA flow over
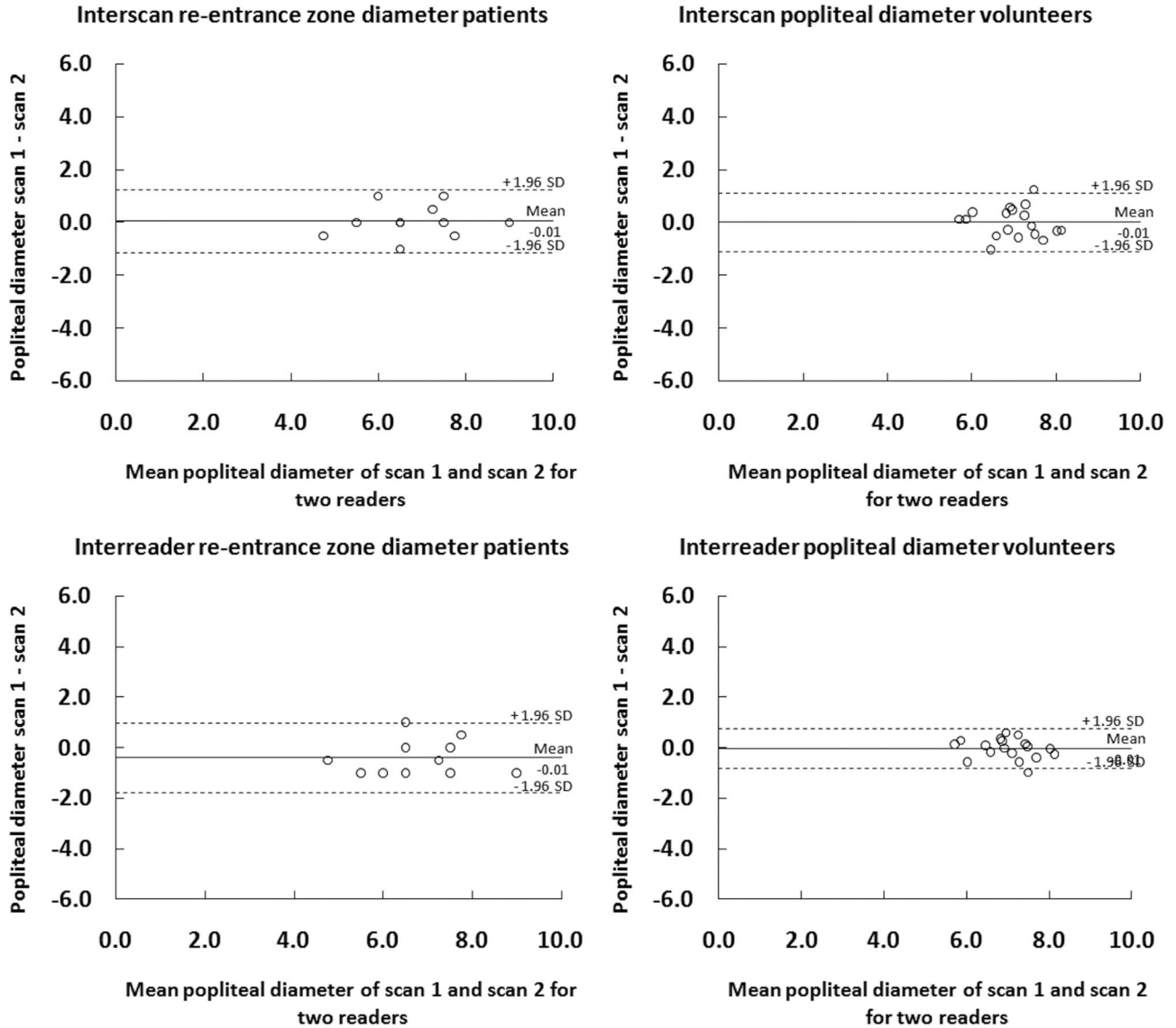
FIGURE 6. Interscan and interreader reproducibility of diameters of the conduit artery near the collateral re-entrance zone in PAD patients and of the popliteal artery in volunteers. Bland-Altman plots showing difference in diameter between scans (interscan) or readers (interreader) (y-axis) against mean vessel diameter (x-axis). Absolute mean difference is represented by the solid line and 95% confidence interval is given by the 2 dashed lines.

time and small differences in scan geometry between the 2 examinations in the subjects.

Dynamic Contrast-Enhanced MRI

In contrast to PCA MRI, the interscan reproducibility of DCE MRI was poor in patients, with a CV and RC evidently larger than the relative and absolute differences between patients and healthy volunteers. This implies that repeated measurements over time cannot provide reliable information on small changes in DCE MRI derived calf muscle perfusion using the imaging protocol described in this study. Reproducibility studies in skeletal muscle are unfortunately scarce. Previous DCE MRI studies in various tumor types and skeletal muscle performed under resting conditions also reported unfavorable reproducibility measures, particularly for muscle tissue.[9,21] In agreement with our study, the AUC parameter appeared to be more reproducible than the corresponding K_i (proportional to

K^{trans} in Ref[19]). In the study by Galbraith et al the flow level of resting state muscle was low and likely prone to large day-to-day variations in the endothelial function (ie, endothelial permeability and bioavailability of nitric oxide).[21,48] Indeed, T1 values, as determined during the precontrast T1 mapping, showed high interscan reproducibility in both patients (mean, T1 578 ± 148 milliseconds; CV, 2.7%; RC, 43 milliseconds; and ICC, 0.99) and healthy volunteers (mean, T1 480 ± 28 milliseconds; CV, 3.1%; RC, 42 milliseconds; and ICC, 0.71), indicating that the technique itself was reproducible. However, the physiologic process we studied was not. To obtain a higher flow level, which better represented physical activity, we used a cuff inflation-deflation protocol to measure muscle perfusion under reactive hyperemia conditions. Application of such a cuff-compression technique is likely to be more reproducible than exercise paradigms, because this paradigm is independent of the patient's compliance, can be standardized, is less hampered by
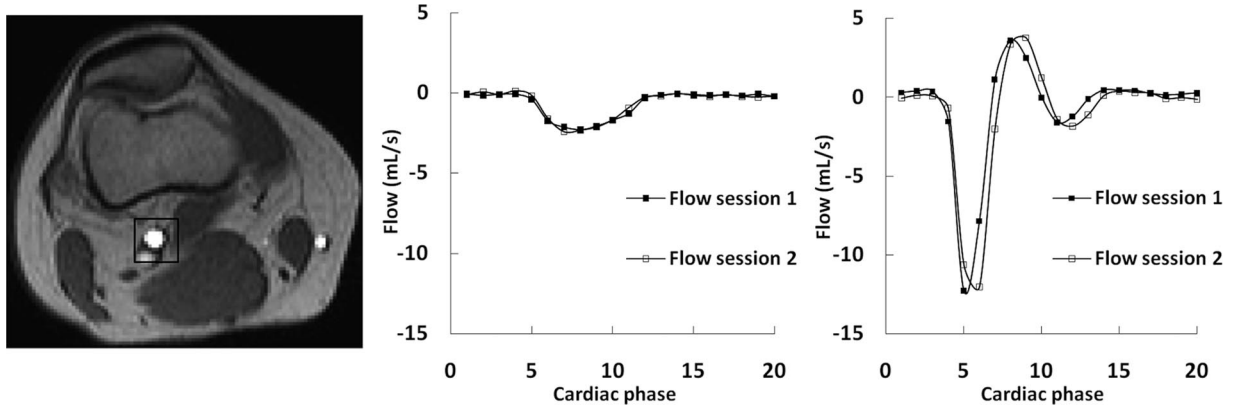
FIGURE 7. PCA modulus image (left panel) of the knee in a 68-year-old patient suffering from Fontaine stage II PAD with a black square marking the popliteal artery. Typical flow waveforms of the popliteal artery are shown in a patient (center panel) and 24-year-old healthy volunteer (right panel) at 2 different time points show excellent reproducibility over time. Note loss of tri-phasic flow waveform and a decrease in peak flow in the patient with PAD compared with the healthy volunteer.

TABLE 4. Reproducibility of PCA MRI in the Popliteal Artery

	Patients (n = 10)	Volunteers (n = 10)
Peak flow (mL/s)	3.15 ± 1.40	9.77 ± 2.06*
Interscan reproducibility		
CV (%)	15.8	6.8
RC (mL/s)	1.4	1.9
ICC (95% CI)	0.94 (0.76–0.98)	0.89 (0.77–0.97)
Interreader reproducibility		
CV (%)	7.0	5.9
RC (mL/s)	0.6	1.6
ICC (95% CI)	0.98 (0.95–0.99)	0.92 (0.51–0.93)

Values are presented as mean ± SD.
*$P < 0.01$.
CV indicates coefficient of variance; RC, repeatability coefficient; ICC, intraclass correlation coefficient; 95% CI, 95% confidence interval; SD, standard deviation.

motion artifacts of the leg, and induces a general reactive hyperemia in all calf muscles in contrast to exercise paradigms, which activate specific calf muscles.[13] Despite these advantages, the interscan reproducibility revealed large day-to-day variations.

Interreader reproducibility proved high, indicating a low reader dependency of the measurement, which is desirable for application in therapy monitoring and follow-up studies.

Blood Oxygen Level-Dependent MRI

Although better than the interscan reproducibility of DCE MRI, the interscan reproducibility for $rT2_{max}$ in BOLD MRI was also found to be poor. TTP, however, was fairly reproducible in both patients and healthy volunteers. Analogous to DCE MRI, the BOLD technique showed good interscan reproducibility, as proven by the interscan reproducibility of T2* relaxation times, prior to the actual BOLD MRI (mean T2*, 24.5 ± 1.2 milliseconds; CV, 3.7%; RC, 2.5 milliseconds; and ICC 0.47 in patients and 23.1 ± 3.5 milliseconds; CV, 12.3%; RC, 8 milliseconds; and ICC, 0.31 in healthy volunteers, respectively), indicating large biologic day-to-day variation in muscle tissue oxygenation, resulting in poor interscan reproducibility for $rT2_{max}$ in the dynamic BOLD measurement. This means that small changes in muscle tissue oxygenation, as reflected by changes in $rT2_{max}$ cannot be measured reliably with BOLD MRI.

Macrovascular Versus Microvascular Reproducibility

In this study, we found that macrovascular flow can be reliably determined by PCA MRI, whereas methods used to measure microvascular function were subject to large interscan variations, with the exception of the TTP in BOLD MRI. These results corroborate to the findings of Wu et al showing variations in the perfusion of the soleus muscle of healthy volunteers of up to 20% within 1 hour using a similar cuff compression method and arterial spin labeling at 3 Tesla.[34]

Our observation of poor microvascular interscan reproducibility is remarkable given the reproducible PA flow, and thus blood supply to calf muscle. There might be 2 underlying reasons for this apparent discrepancy. First, the microcirculation of the calf muscle itself is likely more prone to day-to-day variations than macrovascular flow as the microcirculation and endothelial function are influenced by many intrinsic (ie, hormonal and circadian cycles, insulin supply, shunting and rerouting of blood) and extrinsic (ie, outside temperature, season, time of the day, food, pharmacologic) factors.[49] Many of these factors are susceptible to day-to-day variations and will therefore inevitably negatively impact reproducibility of microvascular function. A second factor that might partly explain our findings is that microvascular function was assessed under reactive hyperemic conditions, whereas the PA flow was measured under resting conditions.

The better interscan reproducibility of BOLD MRI over DCE MRI might be explained by the fact that DCE MRI parameters (Ki and AUC) are determined by processes that occur within a very short period of time (less than 20 seconds) and depend on endothelial function to a large extent (ie, extravasation of contrast agent), whereas TTP for BOLD MRI is a much slower process (taking up to 2 minutes) not depending on endothelial leakage, indicating that the endothelial function has less influence on the results.

Clinical Perspective

Reproducible noninvasive imaging tools are needed for studying the processes of vascular adaptations and collateral development in patients with PAD. Our method can be used to visualize and reproducibly quantify collateral vessel formation over time for monitoring vascular adaptive responses to various treatments in patients with PAD. As interscan reproducibility was evidently better compared with the interreader reproducibility for both artery count and diameter assessment in most cases, it would be advisable to use the same image reader in follow-up studies. Under these conditions,
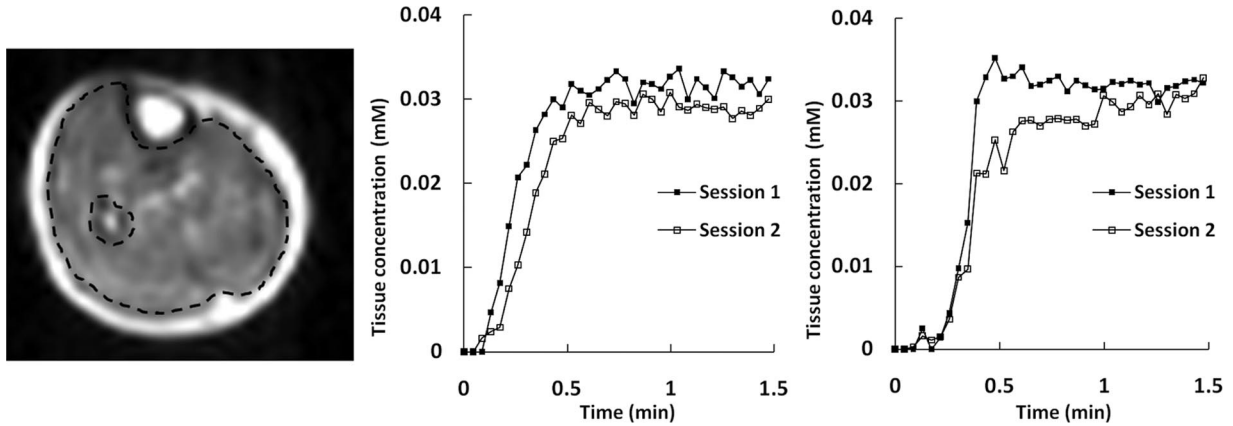
FIGURE 8. Example of DCE image (left panel) in a 68-year-old patient suffering from Fontaine stage II PAD. Reproducibility was determined for a ROI covering the entire muscular volume (area between the black dotted contours). Graphics show the signal intensity converted to contrast agent concentration over time directly after cuff deflation in a PAD patient (center panel) and healthy volunteer (right panel) for both sessions. Note the interscan variability in PAD patients and healthy volunteers.

TABLE 5. Reproducibility of DCE MRI in the Calf

	Patients (n = 8)	Volunteers (n = 10)
Ki (min^{-1})	0.64 ± 0.22	0.84 ± 0.26*
Interscan reproducibility		
CV (%)	50.9	17.7
RC (min^{-1})	0.9	0.4
ICC (95% CI)	0.00 (0.00–0.65)	0.71 (0.22–0.92)
Interreader reproducibility		
CV (%)	6.3	3.5
RC (min^{-1})	0.1	0.1
ICC (95% CI)	0.97 (0.86–0.99)	0.99 (0.95–0.99)
AUC (mMs)	4.18 ± 1.26	3.53 ± 1.24†
Interscan reproducibility		
CV (%)	26.1	10.7
RC (mMs)	3.0	1.0
ICC (95% CI)	0.45 (0.00–0.86)	0.69 (0.17–0.91)
Interreader reproducibility		
CV (%)	4.2	6.2
RC (mMs)	0.5	0.6
ICC (95% CI)	0.98 (0.92–0.99)	0.97 (0.89–0.99)

Values are presented as mean ± SD.
*P = 0.07.
†P = 0.09.
Ki indicates influx constant; CV, coefficient of variance; RC, repeatability coefficient; ICC, intraclass correlation coefficient; 95% CI, 95% confidence interval; AUC, area under the curve; SD, standard deviation.
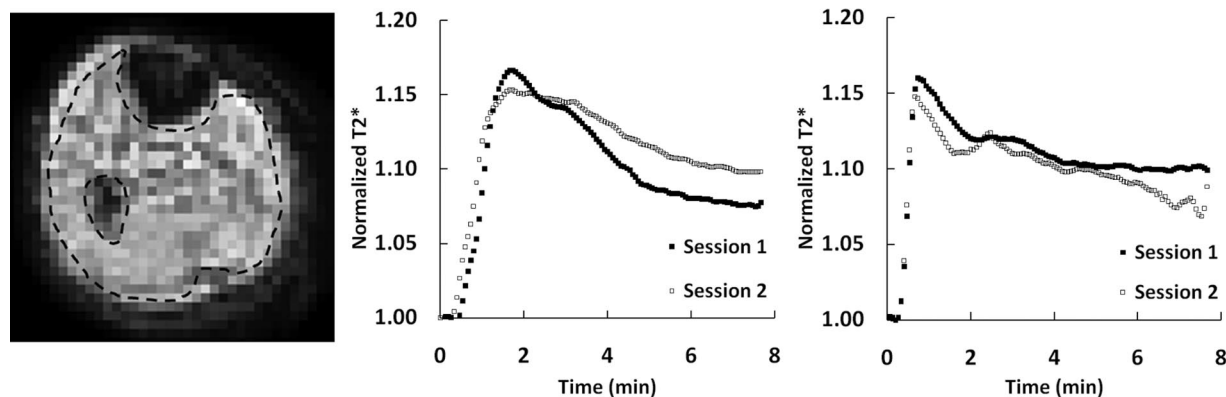
reproducibility, indicating a low observer dependency of the measurements, and short acquisition duration, allow easy implementation of flow measurements combined with routine CE-MRA examinations in clinical practice. Further studies are needed to determine the potential of this technique to discriminate between normal and clinically relevant low flow levels in relation to functional parameters such as walking distance and quality of life.

Taken together, the results of the DCE and BOLD MRI indicate that the perfusion responses in the calf muscles of patients with PAD were slower compared with healthy volunteers. However, detecting perfusion differences between patients and healthy volunteers was not the primary goal of this study. Such observable differences will strongly depend on the type of patients and controls included. Anyhow, this finding demonstrates the potential of these MRI techniques to distinguish between different perfusion levels and supports the findings of previous studies comparing patients and controls. Despite the discriminative ability of microvascular functional MRI, DCE MRI does not appear to be a reliable method to quantify changes in the functional status of the microcirculation over time. Additional studies are required to investigate whether better standardization of patient conditions and/or protocols will improve the reproducibility of functional MRI techniques and to determine the clinical applicability of microvascular MRI to assess skeletal muscle perfusion.

Study Limitations

The presented method for the artery count allows quantification of the total number of arteries in the upper leg, although it cannot differentiate between pre-existing large conduit arteries, muscular branches, and collateral arteries. This method may well be used for follow-up studies evaluating the effectiveness of therapies that stimulate collateral vessel formation, because even a very small increase in the number of collateral arteries, with a caliber exceeding 0.5 mm, will be detectable. Furthermore, review of the source images allows easy identification of the large named arteries in the upper leg.

A comparison between conventional digital subtraction angiography (DSA) and CE-MRA to quantify the number of collaterals would have been useful. Unfortunately, for most patients, no DSA images were available. Previous results of our research group in animal models show that DSA consistently identifies more and smaller collateral arteries.[50] However, in the study by de Lussanet et

the sensitivity of CE-MRA for the detection of new collateral arteries is very high and allows the detection of an increase of more than 1 vessel per plane or an increase of more than 1 mm in diameter of the collateral re-entrance zone beyond measurement error.

At functional level, we demonstrated that PCA MRI can reproducibly determine peak blood flow in the PA and can reliably detect changes in macrovascular blood flow over time. Although our data are not directly comparable to those of previous studies, who mainly focused on mean flow,[16,18] we confirmed the findings of Mohajer et al, by detecting a decrease in blood flow distal to vascular lesions in the SFA in patients.[10] The high interreader

FIGURE 9. Example of BOLD image (left panel) in a 68-year-old patient with Fontaine stage II PAD. Reproducibility was determined for an ROI covering the entire muscular volume (area between the black dotted contours). Graphics show the normalized T_2* over time directly after cuff deflation in a PAD patient (center panel) and healthy volunteer (right panel) for both sessions. Note the large interscan variability in PAD patients (center panel) and healthy volunteers (right panel).

TABLE 6. Reproducibility of BOLD MRI in the Calf

	Patients (n = 8)	Volunteers (n = 10)
rT2max (%)	13.2 ± 6.4	13.3 ± 5.9*
Interscan reproducibility		
CV (%)	26.7	21.5
RC (%)	9.7	7.9
ICC (95% CI)	0.71 (0.13–0.93)	0.79 (0.38–0.94)
Interreader reproducibility		
CV (%)	1.5	4.3
RC (%)	0.5	1.6
ICC (95% CI)	0.99 (0.95–0.99)	0.99 (0.97–0.99)
TTP(s)	116 ± 26.8	60.7 ± 15.9†
Interscan reproducibility		
CV (%)	10.6	15.9
RC (s)	33.8	26.7
ICC (95% CI)	0.80 (0.35–0.96)	0.69 (0.18–0.91)
Interreader reproducibility		
CV (%)	11.3	18.8
RC (s)	36.1	31.4
ICC (95% CI)	0.78 (0.28–0.95)	0.59 (0.01–0.88)

Values are presented as mean ± SD.
*P = 0.97.
†P < 0.01.
rT2$_{max}$ indicates relative change in T2*; CV, coefficient of variance; RC, repeatability coefficient; ICC, intraclass correlation coefficient; 95% CI, 95% confidence interval; TTP, time-to-peak; Sd, standard deviations.

al, it is argued that these small collateral arteries do not add substantially to the blood supply.[50]

In clinical practice, MRA examinations of PAD patients are used to visualize the entire peripheral arterial tree from the infrarenal aorta down to the feet. Although most collaterals of the upper leg are located near the adductor canal as previously found by Wecksell et al,[51] we imaged the entire volume of the thigh for maximal axial coverage. This resulted in increased acquisition duration of the upper leg station (on average, 40–50 seconds instead of the usual 10–15 seconds). Also, we did not assess reproducibility of the measurement in the pelvic and lower leg stations in this study. A future improvement could be the use of a blood pool contrast agent

as this would allow a first-pass CE-MRA of the upper leg using our extended field of view for artery quantification, followed by high-resolution steady-state images of the total peripheral arterial tree for clinical assessment of the peripheral vasculature.[52,53] A disadvantage of this approach is the venous enhancement during the steady state; however, due to the high resolution, easy differentiation between arteries and veins is possible.[52,53]

For analysis of DCE MRI data, we used a standardized VIF. Although an individual VIF could potentially be more accurate, we were not able to identify suitable arteries in the majority of the patients (5 out of 8) and in 2 healthy volunteers. Low spatial resolution most likely explains the failure to identify a suitable artery in these subjects. Although increased spatial resolution might improve the determination of an individual VIF, it would directly worsen the signal-to-noise ratio and the temporal sampling conditions of the rapidly increasing MRI signal. Furthermore, reproducibility measures were even worse in selected cases where an individual VIF could be determined (data not shown).

CONCLUSIONS

In conclusion, quantification of the morphologic vascular status by CE-MRA, as well as PCA MRI to assess macrovascular blood flow proved highly reproducible in both PAD patients and healthy volunteers and might therefore be helpful in studying the development of collateral arteries in PAD patients and in unraveling the mechanisms underlying this process.

Functional assessment of the microvascular status using DCE and BOLD MRI did not prove reproducible and is therefore currently not suitable for clinical monitoring in PAD.

REFERENCES

1. Norgren L, Hiatt WR, Dormandy JA, et al. Inter-society consensus for the management of peripheral arterial disease (TASC II). *J Vasc Surg*. 2007; 45(suppl S):S5–S67.
2. Leng GC, Fowler B, Ernst E. Exercise for intermittent claudication. *Cochrane Database Syst Rev*. 2000:CD000990.
3. Stewart KJ, Hiatt WR, Regensteiner JG, et al. Exercise training for claudication. *N Engl J Med*. 2002;347:1941–1951.
4. Markkanen JE, Rissanen TT, Kivela A, et al. Growth factor-induced therapeutic angiogenesis and arteriogenesis in the heart—gene therapy. *Cardiovasc Res*. 2005;65:656–664.
5. Tammela T, Enholm B, Alitalo K, et al. The biology of vascular endothelial growth factors. *Cardiovasc Res*. 2005;65:550–563.
6. Aghi M, Chiocca EA. Contribution of bone marrow-derived cells to blood vessels in ischemic tissues and tumors. *Mol Ther*. 2005;12:994–1005.

7. Wahlberg E. Angiogenesis and arteriogenesis in limb ischemia. *J Vasc Surg*. 2003;38:198–203.

8. Hiatt WR, Regensteiner JG, Hargarten ME, et al. Benefit of exercise conditioning for patients with peripheral arterial disease. *Circulation*. 1990;81:602–609.

9. Thompson RB, Aviles RJ, Faranesh AZ, et al. Measurement of skeletal muscle perfusion during postischemic reactive hyperemia using contrast-enhanced MRI with a step-input function. *Magn Reson Med*. 2005;54:289–298.

10. Mohajer K, Zhang H, Gurell D, et al. Superficial femoral artery occlusive disease severity correlates with MR cine phase-contrast flow measurements. *J Magn Reson Imaging*. 2006;23:355–360.

11. de Vries M, Nijenhuis RJ, Hoogeveen RM, et al. Contrast-enhanced peripheral MR angiography using SENSE in multiple stations: feasibility study. *J Magn Reson Imaging*. 2005;21:37–45.

12. Leiner T, Kessels AG, Nelemans PJ, et al. Peripheral arterial disease: comparison of color duplex US and contrast-enhanced MR angiography for diagnosis. *Radiology*. 2005;235:699–708.

13. Ledermann HP, Schulte AC, Heidecker HG, et al. Blood oxygenation level-dependent magnetic resonance imaging of the skeletal muscle in patients with peripheral arterial occlusive disease. *Circulation*. 2006;113:2929–2935.

14. de Vries M, de Koning PJ, de Haan MW, et al. Accuracy of semiautomated analysis of 3D contrast-enhanced magnetic resonance angiography for detection and quantification of aortoiliac stenoses. *Invest Radiol*. 2005;40:495–503.

15. Voth M, Haneder S, Huck K, et al. Peripheral magnetic resonance angiography with continuous table movement in combination with high spatial and temporal resolution time-resolved MRA With a total single dose (0.1 mmol/kg) of gadobutrol at 3.0 T. *Invest Radiol* 2009;44:627–633.

16. Meyer RA, Foley JM, Harkema SJ, et al. Magnetic resonance measurement of blood flow in peripheral vessels after acute exercise. *Magn Reson Imaging*. 1993;11:1085–1092.

17. Bakker CJ, Kouwenhoven M, Hartkamp MJ, et al. Accuracy and precision of time-averaged flow as measured by nontriggered 2D phase-contrast MR angiography, a phantom evaluation. *Magn Reson Imaging*. 1995;13:959–965.

18. Klein WM, Bartels LW, Bax L, et al. Magnetic resonance imaging measurement of blood volume flow in peripheral arteries in healthy subjects. *J Vasc Surg*. 2003;38:1060–1066.

19. Prakash A, Garg R, Marcus EN, et al. Faster flow quantification using sensitivity encoding for velocity-encoded cine magnetic resonance imaging: in vitro and in vivo validation. *J Magn Reson Imaging*. 2006;24:676–682.

20. Isbell DC, Epstein FH, Zhong X, et al. Calf muscle perfusion at peak exercise in peripheral arterial disease: measurement by first-pass contrast-enhanced magnetic resonance imaging. *J Magn Reson Imaging*. 2007;25:1013–1020.

21. Galbraith SM, Lodge MA, Taylor NJ, et al. Reproducibility of dynamic contrast-enhanced MRI in human muscle and tumours: comparison of quantitative and semi-quantitative analysis. *NMR Biomed*. 2002;15:132–142.

22. Barrett T, Brechbiel M, Bernardo M, et al. MRI of tumor angiogenesis. *J Magn Reson Imaging*. 2007;26:235–249.

23. Noseworthy MD, Bulte DP, Alfonsi J. BOLD magnetic resonance imaging of skeletal muscle. *Semin Musculoskelet Radiol*. 2003;7:307–315.

24. Duteil S, Wary C, Raynaud JS, et al. Influence of vascular filling and perfusion on BOLD contrast during reactive hyperemia in human skeletal muscle. *Magn Reson Med*. 2006;55:450–454.

25. Baudelet C, Cron GO, Gallez B. Determination of the maturity and functionality of tumor vasculature by MRI: correlation between BOLD-MRI and DCE-MRI using P792 in experimental fibrosarcoma tumors. *Magn Reson Med*. 2006;56:1041–1049.

26. Stainsby JA, Wright GA. Monitoring blood oxygen state in muscle microcirculation with transverse relaxation. *Magn Reson Med*. 2001;45:662–672.

27. Bulte DP, Alfonsi J, Bells S, et al. Vasomodulation of skeletal muscle BOLD signal. *J Magn Reson Imaging*. 2006;24:886–890.

28. Haacke M, Brown R, Thompson M, et al. T1 estimation from SSI measurements at multiple flip angles. In: Haacke M, Brown R, Thompson M, et al, eds. *Magnetic Resonance Imaging: Physical Principles and Sequence Design*. New York, NY: John Willey & Sons, Inc; 1999:654–661.

29. Bland JM, Altman DG. Measurement error. *BMJ*. 1996;312:1654.

30. Jansen JF, Kooi ME, Kessels AG, et al. Reproducibility of quantitative cerebral T2 relaxometry, diffusion tensor imaging, and 1H magnetic resonance spectroscopy at 3.0 Tesla. *Invest Radiol*. 2007;42:327–337.

31. Bland JM, Altman DG. Statistical methods for assessing agreement between two methods of clinical measurement. *Lancet*. 1986;1:307–310.

32. Begelman SM, Jaff MR. Noninvasive diagnostic strategies for peripheral arterial disease. *Cleve Clin J Med*. 2006;73(suppl 4):S22–S29.

33. van Langen H, van Gurp J, Rubbens L. Interobserver variability of ankle-brachial index measurements at rest and post exercise in patients with intermittent claudication. *Vasc Med*. 2009;14:221–226.

34. Wu WC, Wang J, Detre JA, et al. Hyperemic flow heterogeneity within the calf, foot, and forearm measured with continuous arterial spin labeling MRI. *Am J Physiol Heart Circ Physiol*. 2008;294:H2129–H2136.

35. Burchert W, Schellong S, van den Hoff J, et al. Oxygen-15-water PET assessment of muscular blood flow in peripheral vascular disease. *J Nucl Med*. 1997;38:93–98.

36. Bragadeesh T, Sari I, Pascotto M, et al. Detection of peripheral vascular stenosis by assessing skeletal muscle flow reserve. *J Am Coll Cardiol*. 2005;45:780–785.

37. Peetrons P. Ultrasound of muscles. *Eur Radiol*. 2002;12:35–43.

38. Chloros GD, Smerlis NN, Li Z, et al. Noninvasive evaluation of upper-extremity vascular perfusion. *J Hand Surg Am*. 2008;33:591–600.

39. Weber MA, Krix M, Delorme S. Quantitative evaluation of muscle perfusion with CEUS and with MR. *Eur Radiol* 2007;17:2663–2674.

40. Ludman PF, Volterrani M, Clark AL, et al. Skeletal muscle blood flow in heart failure measured by ultrafast computed tomography: validation by comparison with plethysmography. *Cardiovasc Res*. 1993;27:1109–1115.

41. Duet M, Virally M, Bailliart O, et al. Whole-body (201)Tl scintigraphy can detect exercise lower limb perfusion abnormalities in asymptomatic diabetic patients with normal Doppler pressure indices. *Nucl Med Commun*. 2001;22:949–954.

42. Ament W, Lubbers J, Rakhorst G, et al. Skeletal muscle perfusion measured by positron emission tomography during exercise. *Pflugers Arch*. 1998;436:653–658.

43. Fleischer AC, Niermann KJ, Donnelly EF, et al. Sonographic depiction of microvessel perfusion: principles and potential. *J Ultrasound Med*. 2004;23:1499–1506.

44. Carlier PG, Bertoldi D, Baligand C, et al. Muscle blood flow and oxygenation measured by NMR imaging and spectroscopy. *NMR Biomed*. 2006;19:954–967.

45. Lebon V, Brillault-Salvat C, Bloch G, et al. Evidence of muscle BOLD effect revealed by simultaneous interleaved gradient-echo NMRI and myoglobin NMRS during leg ischemia. *Magn Reson Med*. 1998;40:551–558.

46. Diehm N, Kickuth R, Gahl B, et al. Intraobserver and interobserver variability of 64-row computed tomography abdominal aortic aneurysm neck measurements. *J Vasc Surg*. 2007;45:263–268.

47. Sueyoshi E, Sakamoto I, Matsuoka Y, et al. Symptomatic peripheral vascular tree stenosis. Comparison of subtracted and nonsubtracted 3D contrast-enhanced MR angiography with fat suppression. *Acta Radiol*. 2000;41:133–138.

48. Ziegler MA, Distasi MR, Bills RG, et al. Marvels, mysteries, and misconceptions of vascular compensation to peripheral artery occlusion. *Microcirculation*. 2010;17:3–20.

49. Deanfield J, Donald A, Ferri C, et al. Endothelial function and dysfunction. Part I: methodological issues for assessment in the different vascular beds: a statement by the Working Group on Endothelin and Endothelial Factors of the European Society of Hypertension. *J Hypertens*. 2005;23:7–17.

50. de Lussanet QG, van Golde JC, Beets-Tan RG, et al. Magnetic resonance angiography of collateral vessel growth in a rabbit femoral artery ligation model. *NMR Biomed*. 2006;19:77–83.

51. Wecksell MB, Winchester PA, Bush HL Jr, et al. Cross-sectional pattern of collateral vessels in patients with superficial femoral artery occlusion. *Invest Radiol*. 2001;36:422–429.

52. Hadizadeh DR, Gieseke J, Lohmaier SH, et al. Peripheral MR angiography with blood pool contrast agent: prospective intraindividual comparative study of high-spatial-resolution steady-state MR angiography versus standard-resolution first-pass MR angiography and DSA. *Radiology*. 2008;249:701–711.

53. Wang MS, Haynor DR, Wilson GJ, et al. Maximizing contrast-to-noise ratio in ultra-high resolution peripheral MR angiography using a blood pool agent and parallel imaging. *J Magn Reson Imaging*. 2007;26:580–588.